

Electronic Supplementary Information

A computational study of design and performance investigation of Ni-based electrocatalysts for efficient electrocatalytic hydrogen evolution reaction

Jingyi Zou, Xuefeng Ren*

School of Ocean Science and Technology, Dalian University of Technology, Panjin, 124221, China.

E-mail: renxuefeng@dlut.edu.cn

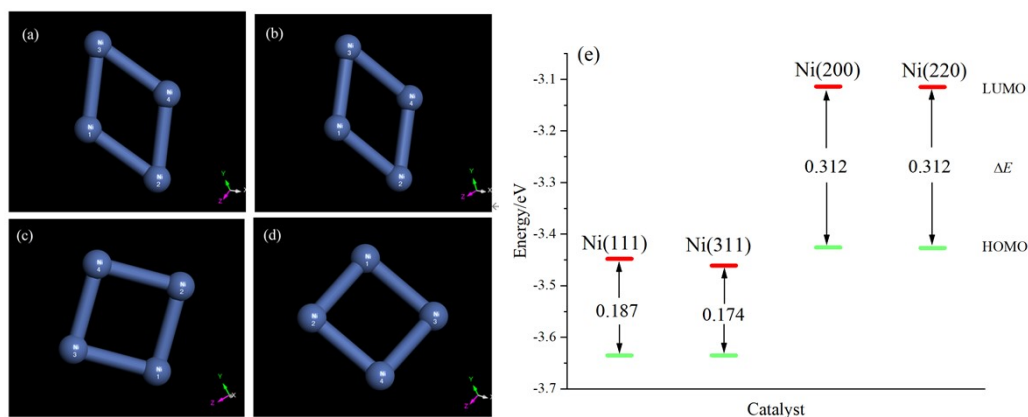


Figure S1. The optimized geometry structure of (a) Ni(111), (b) Ni(311), (c) Ni(200) and (d) Ni(220) crystal planes; E_{HOMO} , E_{LUMO} and ΔE distribution diagram (e) of different Ni crystal planes after optimization.

Table S1. Fukui(-) indices of Ni(111) and Ni(311) crystal planes.

Ni(111)		Ni(311)	
Fukui(-)	Mulliken	Fukui(-)	Mulliken
Ni(1)	0.174	Ni(1)	0.173
Ni(2)	0.328	Ni(2)	0.327
Ni(3)	0.326	Ni(3)	0.326
Ni(4)	0.172	Ni(4)	0.174

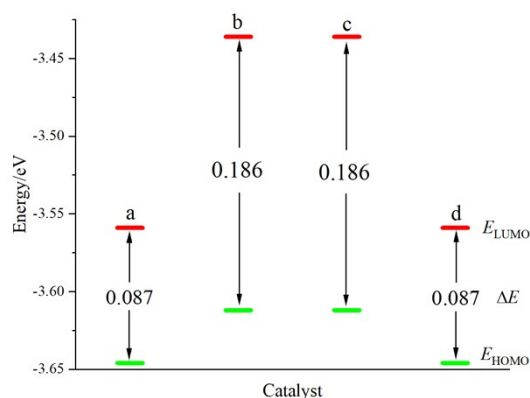


Figure S2. E_{HOMO} , E_{LUMO} and ΔE distribution diagram of unitary-Co-doped Ni(311) crystal planes:

- (a) Ni (311)-2,3,4Ni -1Co; (b) Ni (311)-1,3,4Ni -2Co;
(c) Ni (311)-1,2,4Ni -3Co; (d) Ni (311)-1,2,3Ni -4Co;

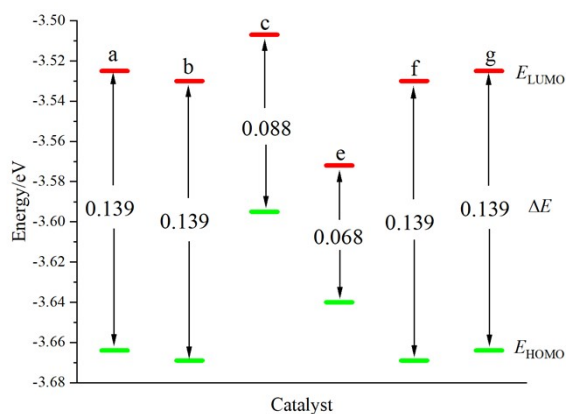


Figure S3. E_{HOMO} , E_{LUMO} and ΔE distribution diagram of binary-Co-doped Ni(311) crystal planes:

- (a) Ni (311) -3,4Ni -1,2Co; (b) Ni (311) -2,4Ni -1,3Co; (c) Ni (311) -2,3Ni -1,4Co;
(d) Ni (311) -1,4Ni -2,3Co; (e) Ni (311) -1,3Ni -2,4Co; (f) Ni (311) -1,2Ni -3,4Co;

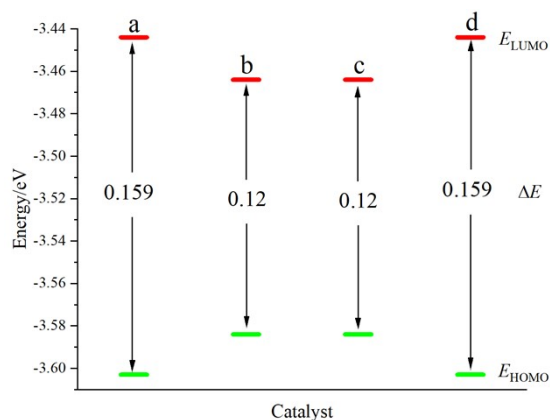


Figure S4. E_{HOMO} , E_{LUMO} and ΔE distribution diagram of ternary-Co-doped Ni(311) crystal planes:

- (a) Ni (311) -4Ni -1,2,3Co; (b) Ni (311)- 3Ni -1,2,4Co;
(c) Ni (311) -2Ni -1,3,4Co; (d) Ni (311) -1Ni -2,3,4Co;

Table S2. Fukui(-) indices of four selected Co-doped Ni(311) crystal planes.

Ni(311)-2,3,4Ni-1Co		Ni(311)-1,2,3Ni-4Co		Ni(311)-2,3Ni-1,4Co		Ni(311)-1,4Ni-2,3Co	
Fukui(-)	Mulliken	Fukui(-)	Mulliken	Fukui(-)	Mulliken	Fukui(-)	Mulliken
Co(1)	0.167	Ni(1)	0.178	Co(1)	0.171	Ni(1)	0.181
Ni(2)	0.328	Ni(2)	0.327	Ni(2)	0.329	Co(2)	0.325
Ni(3)	0.328	Ni(3)	0.329	Ni(3)	0.330	Co(3)	0.313
Ni(4)	0.177	Co(4)	0.167	Co(4)	0.170	Ni(4)	0.181

Table S3. Fukui(-) indices of four selected Co-doped Ni(111) crystal planes.

Ni(111)-2,3,4Ni-1Co		Ni(111)-1,2,3Ni-4Co		Ni(111)-2,3Ni-1,4Co		Ni(111)-1,4Ni-2,3Co	
Fukui(-)	Mulliken	Fukui(-)	Mulliken	Fukui(-)	Mulliken	Fukui(-)	Mulliken
Co(1)	0.169	Ni(1)	0.177	Co(1)	0.170	Ni(1)	0.184
Ni(2)	0.328	Ni(2)	0.328	Ni(2)	0.326	Co(2)	0.320
Ni(3)	0.327	Ni(3)	0.326	Ni(3)	0.329	Co(3)	0.313
Ni(4)	0.176	Co(4)	0.169	Co(4)	0.174	Ni(4)	0.183

Table S4. The calculation process for $E_{\text{H}_2\text{O}_{\text{ads}}}$ (Figure 5) of Co-doped Ni(111) crystal planes.

Catalyst	$E_{\text{slab}+\text{H}_2\text{O}}/\text{Ha}$	$E_{\text{slab}}/\text{Ha}$	$E_{\text{H}_2\text{O}}/\text{Ha}$	$E_{\text{H}_2\text{O}_{\text{ads}}}/\text{Ha}$	$E_{\text{H}_2\text{O}_{\text{ads}}}/\text{eV}$
Ni(111)	-6109.035	-6032.600	-76.388	-0.047	-1.276
Ni(111)-1,4Ni-2,3Co	-5857.880	-5781.433	-76.388	-0.059	-1.617
Ni(111)-2,3Ni-1,4Co	-5857.884	-5781.451	-76.388	-0.045	-1.221
Ni(111)-2,3,4Ni-1Co	-5983.458	-5907.027	-76.388	-0.043	-1.180
Ni(111)-1,2,3Ni-4Co	-5983.461	-5907.027	-76.388	-0.046	-1.259

Table S5. The calculation process for $E_{\text{H}_2\text{O}_{\text{ads}}}$ (Figure 6) of Co-doped Ni(311) crystal planes.

Catalyst	$E_{\text{slab}+\text{H}_2\text{O}}/\text{Ha}$	$E_{\text{slab}}/\text{Ha}$	$E_{\text{H}_2\text{O}}/\text{Ha}$	$E_{\text{H}_2\text{O}_{\text{ads}}}/\text{Ha}$	$E_{\text{H}_2\text{O}_{\text{ads}}}/\text{eV}$
Ni(311)	-6109.005	-6032.600	-76.388	-0.017	-0.458
Ni(311)-1,4Ni-2,3Co	-5857.837	-5781.433	-76.388	-0.016	-0.435
Ni(311)-2,3Ni-1,4Co	-5857.884	-5781.451	-76.388	-0.045	-1.217
Ni(311)-1,2,3Ni-4Co	-5983.430	-5907.027	-76.388	-0.015	-0.421
Ni(311)-2,3,4Ni-1Co (optimal active site at position 2)	-5983.430	-5907.027	-76.388	-0.015	-0.418
Ni(311)-2,3,4Ni-1Co (optimal active site at position 3)	-5983.428	-5907.027	-76.388	-0.013	-0.341

Table S6. The calculation process for ΔG_{H_ads} (Figure 7) of Co-doped Ni(111) crystal planes.

Catalyst	E_{slab+H}/Ha	E_{slab}/Ha	E_{H_2}/Ha	E_{H_ads}/Ha	E_{H_ads}/eV	$\Delta G_{H_ads}/eV$
Ni(111)	-6033.215	-6032.600	-1.164	-0.033	-0.908	-0.668
Ni(111)-1,4Ni-2,3Co	-5782.060	-5781.433	-1.164	-0.045	-1.221	-0.981
Ni(111)-2,3Ni-1,4Co	-5782.063	-5781.451	-1.164	-0.030	-0.816	-0.576
Ni(111)-1,2,3Ni-4Co	-5907.637	-5907.027	-1.164	-0.028	-0.771	-0.531
Ni(111)-2,3,4Ni-1Co	-5907.640	-5907.027	-1.164	-0.031	-0.849	-0.609

Table S7. The calculation process for ΔG_{H_ads} (Figure 8) of Co-doped Ni(311) crystal planes.

Catalyst	E_{slab+H}/Ha	E_{slab}/Ha	E_{H_2}/Ha	E_{H_ads}/Ha	E_{H_ads}/eV	$\Delta G_{H_ads}/eV$
Ni(311)	-6033.211	-6032.600	-1.164	-0.029	-0.780	-0.540
Ni(311)-1,4Ni-2,3Co	-5782.066	-5781.433	-1.164	-0.051	-1.379	-1.139
Ni(311)-2,3Ni-1,4Co	-5782.063	-5781.451	-1.164	-0.030	-0.816	-0.576
Ni(311)-1,2,3Ni-4Co	-5907.637	-5907.027	-1.164	-0.029	-0.779	-0.539
Ni(311)-2,3,4Ni-1Co (optimal active site at position 3)	-5907.637	-5907.027	-1.164	-0.028	-0.773	-0.533
Ni(311)-2,3,4Ni-1Co (optimal active site at position 2)	-5907.640	-5907.027	-1.164	-0.032	-0.858	-0.618

Table S8. The calculation process for $E_{H_2O_ads}$ (Figure 9) of Mo-doped Ni(111)-1,4Ni-2,3Co catalysts.

Catalyst	E_{slab+H_2O}/Ha	E_{slab}/Ha	E_{H_2O}/Ha	$E_{H_2O_ads}/Ha$	$E_{H_2O_ads}/eV$
Ni(111)-1,4Ni-2,3Co	-5857.880	-5781.433	-76.388	-0.059	-1.617
Ni(111)-1Ni-2,3Co-4Mo	-8326.942	-8250.516	-76.388	-0.039	-1.048
Ni(111)-4Ni-2,3Co-1Mo	-8326.923	-8250.516	-76.388	-0.019	-0.510

Table S9. The calculation process for $E_{H_2O_ads}$ (Figure 10) of Mo-doped Ni(311)-2,3Ni-1,4Co catalysts.

Catalyst	E_{slab+H_2O}/Ha	E_{slab}/Ha	E_{H_2O}/Ha	$E_{H_2O_ads}/Ha$	$E_{H_2O_ads}/eV$
Ni(311)-2,3Ni-1,4Co	-5857.884	-5781.451	-76.388	-0.045	-1.217
Ni(311)-2Ni-1,4Co-3Mo	-8326.941	-8250.497	-76.388	-0.056	-1.521
Ni(311)-3Ni-1,4Co-2Mo	-8326.920	-8250.497	-76.388	-0.035	-0.949

Table S10. The calculation process for ΔG_{H_ads} (Figure 11) of Mo-doped Ni(311)-2,3,4Ni-1Co catalysts.

Catalyst	E_{slab+H}/Ha	E_{slab}/Ha	E_{H_2}/Ha	E_{H_ads}/Ha	E_{H_ads}/eV	$\Delta G_{H_ads}/eV$
Ni(311)-2,3,4Ni-1Co	-5907.637	-5907.027	-1.164	-0.028	-0.773	-0.533
Ni(311)-2Ni-1Co-3,4Mo	-10845.76	-10845.16	-1.164	-0.024	-0.655	-0.415
Ni(311)-3Ni-1Co-2,4Mo	-10845.76	-10845.16	-1.164	-0.024	-0.652	-0.412
Ni(311)-4Ni-1Co-2,3Mo	-10845.77	-10845.15	-1.164	-0.032	-0.879	-0.639
Ni(311)-2,3Ni-1Co-4Mo (optimal active site at position 2)	-8376.696	-8376.085	-1.164	-0.029	-0.796	-0.556
Ni(311)-2,3Ni-1Co-4Mo (optimal active site at position 3)	-8376.696	-8376.085	-1.164	-0.029	-0.791	-0.551
Ni(311)-2,4Ni-1Co-3Mo	-8376.697	-8376.075	-1.164	-0.040	-1.097	-0.857
Ni(311)-3,4Ni-1Co-2Mo	-8376.696	-8376.075	-1.164	-0.040	-1.081	-0.841

Table S11. The calculation process for ΔG_{H_ads} (Figure 12) of Mo-doped Ni(111)-1,2,3Ni-4Co catalysts.

Catalyst	E_{slab+H}/Ha	E_{slab}/Ha	E_{H_2}/Ha	E_{H_ads}/Ha	E_{H_ads}/eV	$\Delta G_{H_ads}/eV$
Ni(111)-1,2,3Ni-4Co	-5907.637	-5907.027	-1.164	-0.028	-0.771	-0.531
Ni(111)-1Ni-4Co-2,3Mo	-10845.78	-10845.10	-1.164	-0.096	-2.624	-2.384
Ni(111)-2Ni-4Co-1,3Mo	-10845.77	-10845.16	-1.164	-0.037	-1.002	-0.762
Ni(111)-3Ni-4Co-1,2Mo	-10845.77	-10845.15	-1.164	-0.037	-1.001	-0.761
Ni(111)-1,2Ni-4Co-3Mo	-8376.697	-8376.057	-1.164	-0.058	-1.586	-1.346
Ni(111)-1,3Ni-4Co-2Mo	-8376.703	-8376.086	-1.164	-0.035	-0.943	-0.703
Ni(111)-2,3Ni-4Co-1Mo	-8376.696	-8376.085	-1.164	-0.029	-0.794	-0.554

Table S12. The calculation process for ΔG_{H_ads} (Figure 13) of Mo-doped Ni(311)-1,2,3Ni-4Co catalysts.

Catalyst	E_{slab+H}/Ha	E_{slab}/Ha	E_{H_2}/Ha	E_{H_ads}/Ha	E_{H_ads}/eV	$\Delta G_{H_ads}/eV$
Ni(311)-1,2,3Ni-4Co	-5907.637	-5907.027	-1.164	-0.029	-0.779	-0.539
Ni(311)-1Ni-4Co-2,3Mo	-10845.77	-10845.15	-1.164	-0.045	-1.233	-0.993
Ni(311)-2Ni-4Co-1,3Mo	-10845.76	-10845.15	-1.164	-0.024	-0.658	-0.418
Ni(311)-3Ni-4Co-1,2Mo	-10845.77	-10845.15	-1.164	-0.039	-1.063	-0.823
Ni(311)-1,2Ni-4Co-3Mo	-8376.696	-8376.075	-1.164	-0.040	-1.079	-0.839
Ni(311)-1,3Ni-4Co-2Mo	-8376.696	-8376.075	-1.164	-0.040	-1.077	-0.837
Ni(311)-2,3Ni-4Co-1Mo (optimal active site at position 2)	-8376.696	-8376.085	-1.164	-0.029	-0.790	-0.550
Ni(311)-2,3Ni-4Co-1Mo (optimal active site at position 3)	-8376.693	-8376.085	-1.164	-0.026	-0.715	-0.475

Table S13. ΔG_{H_ads} and $E_{H_2O_ads}$ of the Ni(311) crystal plane before and after doping.

Type	Catalyst	$\Delta G_{H_ads}/eV$	$E_{H_2O_ads}/eV$
Original Catalyst	Ni(311)	-0.540	-0.458
Unitary-doped Catalyst	Ni(311)-2,3Ni-1,4Co	-0.567	-1.217
Binary-doped Catalyst	Ni(311)-2Ni-1,4Co-3Mo	-0.997	-1.521
Unitary -doped Catalyst	Ni(311)-2,3,4Ni-1Co	-0.533	-0.341
Binary-doped Catalyst	Ni(311)-3Ni-1Co-2,4Mo	-0.412	-0.427
Unitary-doped Catalyst	Ni(311)-1,2,3Ni-4Co	-0.539	-0.421
Binary-doped Catalyst	Ni(311)-2,3Ni-4Co-1Mo (optimal active site at position 2)	-0.475	-0.340
Binary-doped Catalyst	Ni(311)-2Ni-4Co-1,3Mo	-0.418	-0.468

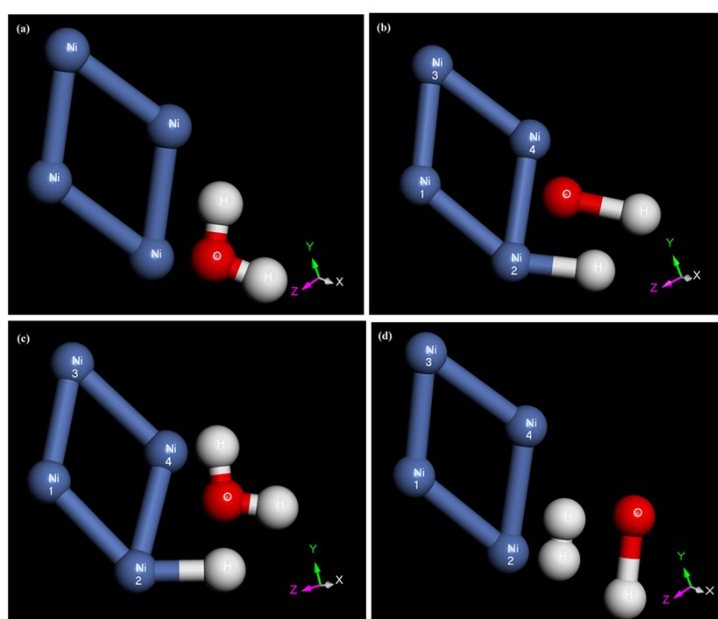


Figure S5. Geometric configurations of reactant, intermediate states, and product in the process of electrocatalytic hydrogen production on Ni(311) with optimal active site at position 2 : (a) Ni(311) + H₂O; (b) Ni(311) - H + H₂; (c) Ni(311) - H + H₂O; (d) Ni(311) + H₂ + H₂O

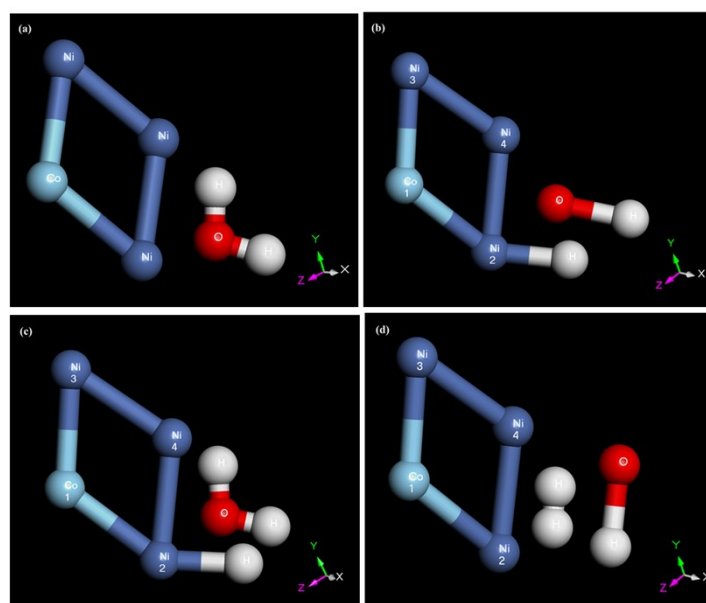


Figure S6. Geometric configurations of reactant, intermediate states, and product in the process of electrocatalytic hydrogen production on Ni(311)-2,3,4Ni-1Co with optimal active site at position 2: (a) Ni(311)-2,3,4Ni-1Co + H₂O; (b) Ni(311)-2,3,4Ni-1Co - H + H₂; (c) Ni(311)-2,3,4Ni-1Co - H + H₂O; (d) Ni(311)-2,3,4Ni-1Co + H₂ + H₂O